Vol 17 No 6, June 2008
1674-1056/2008/17(06)/2208-08

Chinese Physics B

© 2008 Chin. Phys. Soc.
and IOP Publishing Ltd

First-principles calculation of transport property in nano-devices under an external magnetic field*

Chen Jing-Zhe(陈竞哲), Zhang Jin(张 进), and Han Ru-Shan(韩汝珊)

School of Physics, Peking University, Beijing 100871, *China*

(Received 8 October 2007; revised manuscript received 29 November 2007)

The mesoscopic quantum interference phenomenon (QIP) can be observed and behaves as the oscillation of conductance in nano-devices when the external magnetic field changes. Excluding the factor of impurities or defects, specific QIP is determined by the sample geometry. We have improved a first-principles method based on the matrix Green's function and the density functional theory to simulate the transport behaviour of such systems under a magnetic field. We have studied two kinds of QIP: universal conductance fluctuation (UCF) and Aharonov–Bohm effect (A–B effect). We find that the amplitude of UCF is much smaller than the previous theoretical prediction. We have discussed the origin of difference and concluded that due to the failure of ergodic hypothesis, the ensemble statistics is not applicable, and the conductance fluctuation is determined by the flux-dependent density of states (DOSs). We have also studied the relation between the UCF and the structure of sample. For a specific structure, an atomic circle, the A–B effect is observed and the origin of the oscillation is also discussed.

Keywords: first-principles, quantum interference phenomenon (QIP), universal conductance fluctuation (UFC)

PACC: 7115A, 7115M, 7215C

1. Introduction

When the sample size decreases into a characteristic length L_φ, which is the de-phasing length, some mesoscopic quantum coherence phenomena such as universal conductance fluctuation (UCF) and Aharonov–Bohm effect (A–B effect) can be observed in experiments.[1−5] Lee and Stone[6] have analysed the UCF phenomenon and Stone[7] has successfully simulated UCF with Anderson models. Then they focused their attention on the samples with the dimensions in the order of 10 nm (typical dimensions 40 nm×40 nm×800 nm) and concluded that based on the ergodic hypothesis, the amplitude of UCF in mesoscopic systems was in the order of $G_0 = 2e^2/h$, no matter what the structure was.[8] Nowadays, with the rapid development of nano-technology, molecular nano-devices have aroused more and more interest, and some experiments have proved the magnetoresistance fluctuation in them when the sample size is comparable with L_φ, but with much smaller amplitude.[9−18] The samples are all quasi-1D nano-devices which have a long mean free path, e.g. it can be several nanometres for atomic chains and even several microns for some carbon nanotubes.[19] The reduction in number of scattering changes not only the diffusion, but also the transport mechanism. In this nano-limit, UCF behaves differently. Firstly, the amplitude of UCF decreases sharply. Secondly, with a few defects and impurities, the randomness of statistical sample disappears. Finally, the curve of UCF is flux-dependent, and the frequency of oscillation increases with the flux. All the above properties show that the theory of general UCF is not applicable any more, and the quasi-ballistic interference theory is needed to explain the effects.

2. Calculation model

A first principles method which combines the matrix Green's function and density functional theory together (GF+DFT), has gained rapid progress recently in the field of electron coherent transport.[20−24] It succeeded in calculating the conductance of a molecular device including hundreds of atoms between two semi-infinite electrodes. Based on it, we will introduce a method by which the conductance of nano-devices under a magnetic field can be calculated. (Similar work about megetoresistance fluctuation in nano-devices is done by Hod *et al*[25]).

*Project supported by the National Natural Science Foundation of China (Grant Nos 90207009, 90206048 and 90406014).

Our theoretical basis is the Landauer approach in which the transport is considered as a consequent of incident carrier flux and the system conductance is described with a transport coefficient. We consider a long quasi-1D metal wire connected through tunnel barriers with a source lead and a drain lead of the same material (see Fig.1). A local circular perpendicular magnetic field is applied to the region of central device. The Hamiltonian of device is calculated with the density functional theory (DFT), and the electron–phonon interaction is neglected.

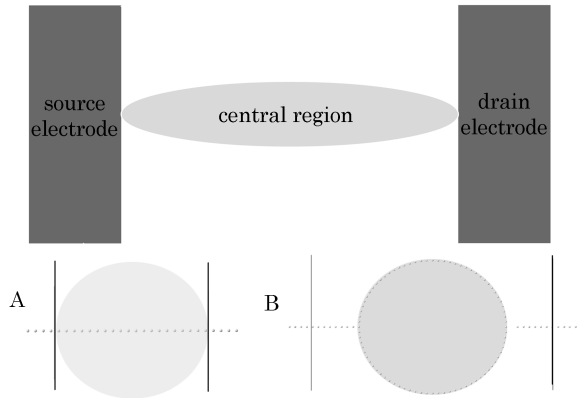


Fig.1. Calculation model, in which two semi-infinite electrodes are connected to a central region where there exists an applied local circular magnetic field perpendicular to the paper. In this paper, we adopt (A) quasi-1D metal chain and (B) metal atomic circle as our samples.

3. The formulas of current and conductance

Let us consider a general scattering formalism for a simple two-terminal model. The transport behaviour is described by the scattering matrix

$$S = \begin{pmatrix} S_{11} & S_{12} \\ S_{21} & S_{22} \end{pmatrix},$$

where $S_{\alpha\beta}$ is the $N_\alpha \times N_\beta$ matrix whose components $(S_{\alpha\beta})_{mn}$ are the ratio between the outgoing amplitude in mode n in lead α and the incoming amplitude in mode m in lead β.

We define $a^+_{n\alpha}(\varepsilon)$ and $a_{n\alpha}(\varepsilon)$ as the creation and annihilation operators on mode n in lead α, and also $b^+_{m\beta}(\varepsilon)$ and $b_{m\beta}(\varepsilon)$ as the creation and annihilation operators on mode m in lead β. Then we have

$$b_{m\alpha} = \sum_{n\beta} (S_{\alpha\beta})_{mn} a_{n\beta}. \tag{1}$$

The current in mode m in lead α is given by

$$I_{m\alpha} = \frac{2e}{h} \int_{-\infty}^{+\infty} \mathrm{d}\varepsilon (\langle a^+_{m\alpha} a_{m\alpha} \rangle - \langle b^+_{m\alpha} b_{m\alpha} \rangle).$$

According to expression (1), we have

$$\begin{aligned} \langle b^+_{m\alpha} b_{m\alpha} \rangle &= \sum_n |S_{\alpha\alpha}|^2 \langle a^+_{n\partial} a_{n\alpha} \rangle \\ &\quad + \sum_n |S_{\alpha\beta}|^2 \left\langle a^+_{n\beta} a_{n\beta} \right\rangle \\ &= \sum_n |S_{\alpha\alpha}|^2 f_\alpha + \sum_n |S_{\alpha\beta}|^2 f_\beta, \end{aligned}$$

where f_α and f_β are the Fermi distribution functions in leads α and β

Considering all the modes, we obtain the total current as

$$I = \frac{2e}{h} \int_{-\infty}^{+\infty} \mathrm{d}\varepsilon (N_1 - R_{11}) f_1 - T_{12} f_2,$$

where $R_{11} = \mathrm{Tr}(S^+_{11} S_{11})$, $T_{12} = \mathrm{Tr}(S^+_{12} S_{12})$, and N_1 is the number of modes in lead α. Unitarity of the scattering matrix (which is required by current conservation) ensures that $\mathrm{Tr}(S^+_{11} S_{11}) + \mathrm{Tr}(S^+_{12} S_{12}) = 1$. Therefore, taking the trace over all modes yields $T_{12} + R_{11} = N_1$, and thus

$$I = \frac{2e}{h} \int_{-\infty}^{+\infty} \mathrm{d}\varepsilon (f_1 - f_2) T_{12}. \tag{2}$$

Take the approximation in which the temperature is absolutely zero and electrodes are infinite in size, then we can write expression (2) as

$$I = \frac{2e}{h} \int_{\mu - eV/2}^{\mu + eV/2} \mathrm{d}\varepsilon T_{12},$$

where μ is the chemical potential of the electrode in equilibrium and V is the bias voltage:
when V is small, we can use this formalism

$$G = \frac{2e^2}{h} T(E_f).$$

The transmission coefficient is calculated by the Fisher-Lee relation

$$T(E) = \mathrm{Tr}(\Gamma_1 G^{\mathrm{R}} \Gamma_2 G^{\mathrm{A}}).$$

The retarded Green's function is:

$$G^{\mathrm{R}} = ((E + \mathrm{i}\eta) S - F - \Sigma_1 - \Sigma_2)^{-1},$$

where $\Sigma_{1,2} = \tau_{1,2} g^{\mathrm{R}}_{1,2} \tau^{+}_{1,2}$ with $\tau_{1,2}$ is the coupling Hamiltonian between the central device and the electrode and $g^{\mathrm{R}}_{1,2}$ being the retarded surface Green's function of the electrode $\Gamma_{1,2} = \mathrm{i}(\Sigma^{\mathrm{R}}_{1,2} - \Sigma^{\mathrm{A}}_{1,2})$; E is the energy; S and F are the overlap matrix and Fock matrix of periodic boundary condition (PBC) structure.

4. Fock matrix under an external magnetic field

We write the Fock matrix as

$$F = \frac{1}{2m}(P + eA)^2 + V_{\mathrm{core}} + V_{\mathrm{Hartree}} + V_{\mathrm{xc}} + \mu BS,$$

where μ is the spin magnetic moment. Coulomb gauge is adopted and the magnetic vector potential $\boldsymbol{A}$ is defined as

$$\boldsymbol{A} = \frac{1}{2}\boldsymbol{B} \times \boldsymbol{r}.$$

Let $\boldsymbol{r} = \boldsymbol{R} + \boldsymbol{r}'$, where $\boldsymbol{R}$ is the coordinates of atom, and $\boldsymbol{r}'$ is the relative coordinates. Assuming that the direction of the magnetic field is parallel to z axis, the kinetic item can be written as:

$$F^{\mathrm{kinetic}} = \frac{1}{2m}(P^2 + eB(l_z + L_z) + \frac{e^2B^2}{4}(x^2 + y^2 + X^2 + Y^2 + 2xX + 2yY)),$$

where

$$l_z = (xP_y - yP_x),$$
$$L_z = (XP_y - YP_x),$$

x, y, z and X, Y, Z are the components of $\boldsymbol{r}'$ and $\boldsymbol{R}$ respectively.

The electrodes will be influenced by the magnetic vector potential. In this region,

$$\boldsymbol{A} = \frac{1}{2}\boldsymbol{B} \times \boldsymbol{r}\frac{|\boldsymbol{r}_0|^2}{|\boldsymbol{r}|^2},$$

where r_0 is the radius of the magnetic field scope. Use the gauge invariant Gauss-type basis:

$$|\varphi\rangle = cX^l Y^m Z^n e^{-\alpha r^2 - \mathrm{i}\boldsymbol{A}\cdot\boldsymbol{r}},$$

and define the overlap integral as

$$\langle \varphi_i \mid \varphi_j \rangle = || \, l_j, m_j, n_j \rangle \,,$$

then we will have

$$\langle \varphi_i | l_z | \, \varphi_j \rangle = A_x || \, l_j, m_j + 1, n_j \rangle - A_y || \, l_j + 1, m_j, n_j \rangle - \mathrm{i}(m_j || \, l_j + 1, m_j - 1, n_j \rangle - l_j || \, l_j - 1, m_j + 1, n_j \rangle),$$
$$\langle \varphi_i | L_z | \, \varphi_j \rangle = (A_x Y_j - A_y X_j) || \, l_j, m_j, n_j \rangle \,,$$
$$-\mathrm{i}(X_j m_j || \, l_j, m_j - 1, n_j \rangle - Y_j l_j || \, l_j - 1, m_j, n_j \rangle - 2X_j \alpha_j || \, l_j, m_j + 1, n_j \rangle + 2Y_j \alpha_j || \, l_j + 1, m_j, n \rangle),$$

$$\langle \varphi_i | x^2 | \, \varphi_j \rangle = || \, l_j + 2, m_j, n_j \rangle \,,$$

and

$$\langle \varphi_i | xX | \, \varphi_j \rangle = X || \, l_j + 1, m_j, n_j \rangle \,.$$

London approximation is used to calculate the integral,[26,27]

$$\langle \varphi_i | \varphi_j \rangle = \langle \phi_i | \phi_j \rangle \, \mathrm{e}^{iL_{ij}},$$

where, $|\phi\rangle = cX^l Y^m Z^n \mathrm{e}^{-\alpha r^2}$ and $L_{i,j} = \frac{1}{2}(\boldsymbol{A}_j - \boldsymbol{A}_i) \cdot (\boldsymbol{R}_i + \boldsymbol{R}_j)$.

5. The treatment of the electrodes

In the region of electrodes, the magnetic vector potential decays slowly with the ratio $\frac{1}{r}$ and it is difficult to deal with the magnetic vector potential far away from the molecular region. We assume that there exists an annular magnetic field in the region of electrodes. It is parallel to the magnetic field in molecular region with an inverse direction, so the magnetic vector potential can decay to zero out of some scope. And the calculation results of UCF can reach convergence when the magnetic field in the regions of electrodes is weak enough.

In the regions of electrodes, we use this formula:

$$\boldsymbol{A} = \frac{1}{2}\boldsymbol{B}_{\text{eff}} \times \boldsymbol{r},$$

where

$$\boldsymbol{B}_{\text{eff}} = (|\boldsymbol{r}_0|^2\boldsymbol{B} + (\boldsymbol{r}^2 - \boldsymbol{r}_0^2)\boldsymbol{B}_{\text{inv}})/|\boldsymbol{r}|^2.$$

For the case $|\boldsymbol{R}| \gg |\boldsymbol{r}'|$, we can replace $\boldsymbol{r}$ with $\boldsymbol{R}$. Then the calculation of the Fock matrix element is carried out in a way similar to the former.

Within the regions, we have

$$\begin{aligned} F &= F_0 + F_{\text{m}} \\ \tau &= ES - T_0 - T_{\text{m}}, \end{aligned} \tag{3}$$

where F_0 and T_0 are respectively the on-site and the coupled Hamiltonian matrices of two cells (a cell is a unit including four atoms in the paper), which can be calculated with the PBC calculation by the Gaussian package. Meanwhile, F_{m} and T_{m} are the on-site and the coupled Hamiltonian matrices induced by the magnetic field respectively.

The retarded surface Green's function of the electrode and the self-energy are respectively

$$g_{\text{s}}^{\text{R}} = (ES - F - \Sigma + \text{i}0^+)^{-1}, \tag{4}$$

and

$$\Sigma = \tau g_{\text{s}}^{\text{R}} \tau^+.$$

With Eqs.(3) and (4), the self-energy can be solved in an iteratively procedure.

We should point out that the Fermi level of the electrode is calculated as below:

$$N = \int_{-\infty}^{E_{\text{f}}} \text{DOS}(E)\text{d}E,$$

where N is the total number of electrons. And the density of states is calculated from the formula $\text{DOS}(E) = -\frac{1}{\pi}\text{Tr}(\text{Im}(G^{\text{R}}(E)S))$. The Fermi level is not affected by the magnetic field because the magnetic field is applied only to the region of the molecule.

6. Results and analysis

Figure 2(c) shows that the UCF feature of a Na chain which includes 320 cells. (In the appendix we will introduce the extended method of dealing with a big system including thousands of atoms.) The bond-length is 0.330 nm after energy optimization. In this figure Φ is the flux through the scope of electron cloud and the radius of atom is used as the width of this scope (0.186 nm for Na). The Fermi level of Na chain is –2.81 eV. The conductance fluctuates with an amplitude in the order of $0.001G_0$.We also obtain the approximate data for the samples of quasi-1D Au, Li chains.[28] The decrease of amplitude does not accord with the prediction by Stone, $\delta G/G_{\text{av}} \propto N_{\text{c}}^{-0.3}$, in which G_{av} is the average conductance and N_{c} is the number of transport channels. This prediction is suitable for the situation $N_{\text{c}} \gg 1$, but not for nano-devices with only several channels. In such a situation, some basic viewpoints and hypotheses are not valid. General UCF theory is based on a quasi classical model, in which there exist many elastic scattering processes during transport and the electrons keep the memory of phase. Each electron has many possible paths and all the paths construct a statistical ensemble which satisfies the ergodic hypothesis. There are many impurities and defects in samples which behave as scattering centres, and scattering processes are determined by their configurations. In nano-devices, there may be few or even no impurities and defects, and also due to geometry confinement the number of elastic scattering progresses sharply decreases. We also notice that the magnetic fluxes through the sample are much smaller than the quantum magnetic flux $\Phi_0 = h/e$ under an available magnetic field. The ergodic hypothesis in the general UCF theory does not hold true and the ensemble average is not a good explanation any more. So, we should view the UCF effect in nano-devices from a new perspective.

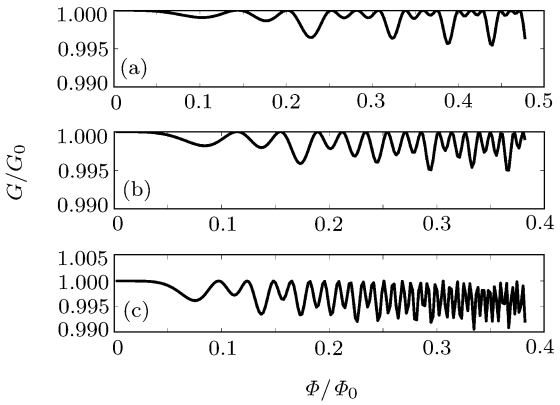


Fig.2. UCF feature of Na chain with 80 (a), 160 (b), and 320 (c) cells in the central region. (In this paper, one cell includes four atoms.)

We conclude that the local magnetic field weakly confines the electrons in a molecular region. In a pure 1D system, a perpendicular magnetic field does not affect the conduction, while it is a little different in

a quasi-1D system. According to classical model, in a magnetic field free electrons have a circular motion with a radius in real space named as Landau radius. The Landau radius is often much bigger than the sample size in an available magnetic field. However, due to the boundary scattering, the electrons will experience a longer path when passing the central region. Then equally, we can view it as a 'weak localization' in a quasi ballistic conduction. In an ultra-high field condition, the electrons will be confined in the molecular region and there are very high potential barriers on the molecular edges, and the DOS will be a series of discrete peaks. And as far as an available magnetic field, the DOS will increase a series of restricted levels, which are approximately equal to the molecular levels.

In the following, we use a simple model to estimate the change of DOS. We divide the total Hamiltonian into three parts, i.e. $H = H_0 + \Sigma_{\rm e} + \Sigma_{\rm m}$, where H_0 is the Hamiltonian under zero magnetic field, $\Sigma_{\rm e}$ is the electrode self-energy and $\Sigma_{\rm m}$ is the flux-related Hamiltonian.

With the Dyson equation, we have

$$G_0 = (ES - H_0 + {\rm i}0^+)^{-1},$$

$$G_1 = G_0 + G_0\Sigma_{\rm e}G_0 + G_0\Sigma_{\rm e}G_0\Sigma_{\rm e}G_0 + \cdots,$$

$$\begin{aligned} G =& G_0 + G_0\Sigma_{\rm e}G_0 + G_0\Sigma_{\rm m}G_0 + G_0\Sigma_{\rm e}G_0\Sigma_{\rm e}G_0 \\ &+ G_0\Sigma_{\rm m}G_0\Sigma_{\rm m}G_0 + G_0\Sigma_{\rm e}G_0\Sigma_{\rm m}G_0 \\ &+ G_0\Sigma_{\rm m}G_0\Sigma_{\rm e}G_0 + \cdots, \end{aligned}$$

$$\begin{aligned} \Delta{\rm DOS} &= -\frac{1}{\pi}{\rm Im}({\rm Tr}(\Delta GS)) \\ &= -\frac{1}{\pi}{\rm Im}({\rm Tr}((G - G_1)S)) \\ &= -\frac{1}{\pi}{\rm Im}({\rm Tr}((G_0\Sigma_{\rm m}G_0 \\ &\quad + G_0\Sigma_{\rm m}G_0\Sigma_{\rm m}G_0 + G_0\Sigma_{\rm e}G_0\Sigma_{\rm m}G_0 \\ &\quad + G_0\Sigma_{\rm m}G_0\Sigma_{\rm e}G_0 + \cdots)S), \end{aligned}$$

where $\Sigma_{\rm m}$ includes a pure imaginary matrix, $\Sigma_{\rm m1} = \dfrac{eB}{2m}(l_z + L_z)$, and a real matrix, $\Sigma_{\rm m2} = \dfrac{e^2B^2}{8m}(x^2 + y^2 + X^2 + Y^2 + 2xX + 2yY)$. According to the hermiticity of Hamiltonian, we know that G_0 and $\Sigma_{\rm m1}$ are antisymmetric matrices, while $\Sigma_{\rm m2}$ and $\Sigma_{\rm e}$ are symmetric matrices. It is easy to prove that the trace of the product of a symmetric matrix and an antisymmetric matrix is zero. So the corresponding ΔDOS with the first order perturbation is $-\dfrac{1}{\pi}{\rm Im}({\rm Tr}(G_0\Sigma_{\rm m2}G_0S))$. And $\Sigma_{\rm m2}$ is often much smaller than $\Sigma_{\rm m1}$ under an available magnetic field.

We take the second order perturbation of G into account, then

$$\begin{aligned} \Delta{\rm DOS} = -\frac{1}{\pi}{\rm Im}({\rm Tr}((&G_0\Sigma_{\rm m2}G_0 + G_0\Sigma_{\rm m1}G_0\Sigma_{\rm m1}G_0 \\ &+ G_0\Sigma_{\rm m2}G_0\Sigma_{\rm m2}G_0 + G_0\Sigma_{\rm m2}G_0\Sigma_{\rm e}G_0S \\ &+ G_0\Sigma_{\rm e}G_0\Sigma_{\rm m2}G_0)S)). \end{aligned}$$

We note that $\Sigma_{\rm m1}$ is linear with B and $\Sigma_{\rm m2}$ is linear with B^2, so we have $\Delta{\rm DO}S \propto B^2$. Meanwhile, G_0 is a pure imaginary impulse function matrix when $E \sim \varepsilon_i, i = 1, 2, \cdots, N$, where ε_i is the molecular level. So the DOS reaches a maximum at a molecular level.

Besides the fluctuation of conductance, another effect induced by the magnetic field is the energy floating. The interaction between the orbital angular momentum and the magnetic field, $\Sigma_{\rm m1}$, makes every level split into n levels, where n is the quantum number of the orbital angular momentum (as to the samples in this paper, $\Sigma_{\rm m1}$ is small, for they are all 's' metals). The item $\Sigma_{\rm m2}$ leads to the energy floating, and the floating scale is linear with Φ^2 for atomic chains. Here, $\Phi = Br_{\rm A}L$, where $r_{\rm A}$ is the radius of atom and L is the length of central region.

The UCF is directly related to the fluctuation of DOS because there is a resonance between the Blöch wave from electrodes and the standing wave constrained by magnetic field when the Fermi level is located at one of the molecular levels. Figures 2(a), 2(b), 2(c) show the UCF curves of Na chain including 80, 160, 320 cells, respectively. As we explained above, one oscillation occurs when the DOS floating exceeds the energy interval between two molecular levels, ΔE. We let the values of ΔE for these samples be ε, $\varepsilon/2$, and $\varepsilon/4$, and we assume that the energy floating satisfies $L_{\rm f} = \alpha\Phi^2$ under a weak magnetic field. Thus the number of oscillations has the relation $N_{\rm osc} = \dfrac{L_{\rm f}}{\Delta E} = \dfrac{\alpha\Phi^2}{\Delta E}$. In Fig.2, the numbers of oscillations in Figs.2(a), 2(b), and 2(c) when $\Phi \leq 0.4\Phi_0$ are 7, 13, and 25 respectively, which well match with our explanation. And due to the fact that the energy floating is linear with Φ^2, we also notice that in each UCF curve the frequency of fluctuation increases with the magnetic field.

7. Comparison and discussion

We also simulate the cases of different structures. The results show that the UCF feature is a charac-

ter of sample structure. Figure 3 displays the UCF curves for four structures: a periodic structure, two kinds of dimer structure, and a zigzag structure. They have different shapes but with the same amplitudes, showing that the UFC amplitude is not sensitive to the sample structure, but to a characteristic size of the sample. In these quasi-1D structures, only the back-scattering takes effect in interference, the flux through the closed area of different Feynman paths is very small. Below, we will discuss a specific structure, i.e. an atomic circle, in which the flux is relatively great and the conductance curve exhibits oscillations with a much bigger amplitude.

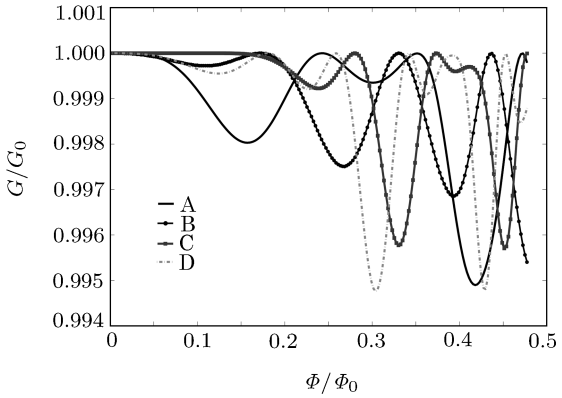


Fig.3. UCF feature for Na chains of different structures, i.e. dimer structure with a displacement 0.001 nm (A), dimer structure with a displacement 0.005 nm (B), zigzag chain with an angle of 5° (C), and periodic Na chain (D).

Figure 4 shows the conductance behaviour of an Au circle and a Na circle. The sample of Au circle includes 100 cells and the sample of Na circle has 200 cells. Periodic conductance oscillations are observed and the period well matches the quantum magnetic flux. Different from the cases of metal chains, the conductance of the circles fluctuates with a much greater amplitude. It is because the interference between the Aharonov–Bohm waves from upper arc and down arc occurs, and the effects generated by back scattering are smeared off. The Fourier analysis shows that there is a $\Phi_0/2$ period also, which is the typical feature of weak localization (WL) effects. The origin is the interference between the clockwise and the anticlockwise Aharonov–Bohm waves propagating the whole circle.

In the experiment of A–B effect which was completed in the 1980s, the sample was an Au circle with a diameter of 820 nm and a width of 40 nm.[3] The result showed that there were two periods in the magnetoresitance curve, i.e. Φ_0 and $\Phi_0/2$. The fluctuation with a period Φ_0 disappears in a high magnetic field. Altshuler claimed that it was because the inner circle and the outer circle had different contour areas. We notice in our results that the amplitude of fluctuation hardly decreases at a high magnetic field, for the atomic circle is the thinnest sample and the difference between different paths can be neglected. The result of calculation provides a strong support for that explanation.

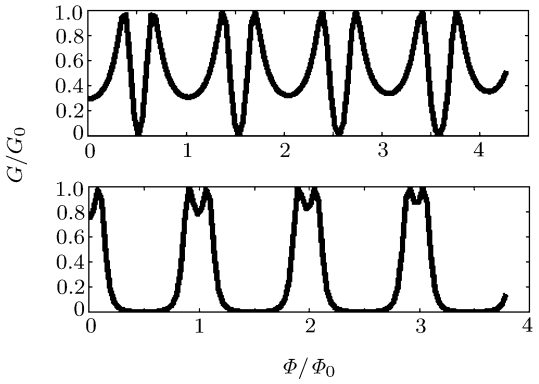


Fig.4. The upper panel shows the conductance oscillation of an Au circle that has 100 cells and a bond-length of 0.2733 nm. The bottom panel is for the case of a Na circle that has 200 cells and a bond-length of 0.330 nm.

We can see in Fig.4 that there are two valleys with different widths in a Φ_0 period. The ratio between them is determined by the coupling with the electrodes.[25] So the fluctuation of conductance in circular devices is very useful because the transport property can be controlled manually by modulating an external magnetic field and the coupling with the electrodes. Therefore it is a possible way to design the molecular logic gate devices in the future.

In conclusion, the QIP in nano-devices including UCF and A–B effect show different properties from those in meososcopic systems. In this paper, we introduce the method in detail which is used to investigate the transport behaviour in nano-devices and by using it we investigate the UCF in metal atomic chains and the A–B effect in atomic circles. Some new physical implications are analysed and discussed, and the flux-related DOS is found to be a key factor.

Appendix

We develop an extended Hamiltonian method to calculate a system including thousands of atoms, much bigger than the number of atoms the Gaussian package can deal with now. It is appropriate for periodic systems, such as chains or circles. In these systems,

the Hamiltonian matrix can be written as

$$H = \begin{pmatrix} H_{\mathrm{LL}} & H_{\mathrm{LC}} & \\ H_{\mathrm{CL}} & H_{\mathrm{CC}} & H_{\mathrm{CR}} \\ & H_{\mathrm{RC}} & H_{\mathrm{RR}} \end{pmatrix},$$

where L, C and R represent the left electrode, the central molecular region, and the right electrode respectively. And H_{CC} has the following form:

$$H_{\mathrm{CC}} = \begin{pmatrix} H_{11} & H_{12} & & & & H_{1N} \\ H_{21} & H_{22} & H_{23} & & & \\ & \ddots & \ddots & \ddots & & \\ & H_{N-2N-3} & H_{N-2N-2} & H_{N-2N-1} & & \\ & & H_{N-1N-2} & H_{N-1N-1} & H_{N-1N} & \\ H_{N1} & & & H_{NN-1} & H_{NN} & \end{pmatrix}.$$

For a periodic system, all the information in the Hamiltonian matrix can be described as three matrices, i.e. T, H_{mm} and H_{mm-1} $(1 \leq m \leq N)$, where H_{mm} is the on-site Hamiltonian matrix, $H_{mm-1}$is the coupled Hamiltonian matrix of adjacent cells, and T is the transformation matrix between the two adjacent cells. T is a unit matrix in the case of a chain, and a rotary group representation matrix in the case of a circle.

Different solutions are adopted to calculate H_{mm} and H_{mm-1} in the case of a chain or a circle. For a chain, the strict Hamiltonian matrix can be calculated by the Gaussian package under PBC, and for a circle, we should calculate a finite arc including a cell and some edge atoms. We keep adding edge atoms on until the electronic potential they generate on the cell hardly change, and approximately we use the potential on the cell generated by the edge atoms to replace that generated by a complete circle. We calculate the total Hamiltonian matrix and then extract the Hamiltonian matrix of the cell as H_{mm} and H_{mm-1}. And T can be calculated by the basis information strictly.

In the next step the Hamiltonian matrix of the electrode is calculated. We need to calculate a semi-infinite chain with the GF self-consistent method.[22,23] In the case of a circle, a finite arc connected to a semi-infinite chain (Part A in Fig.5) should be calculated additionally. To approach the true electronic potential, we also include some edge atoms in the arc and extract the Hamiltonian matrix of Part A out of the total Hamiltonian.

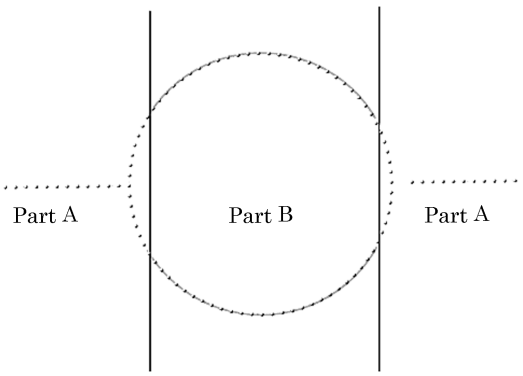


Fig.5. Diagram of the extended method.

Because of many atoms in the sample, we assume that the Hamiltonian of the cell far away from electrodes is equal to that of the cell in a pure circle. So we replace the Hamiltonian matrix of Part B in Fig.5 with the same part for the Hamiltonian matrix of extended molecule. Finally, the Hamiltonian matrix of Part A and that of Part B are combined together to calculate the total Green's function.

References

[1] Webb R A, Washburn S and Umbach C P 1988 *Phys. Rev.* B **37** 8455

[2] Tonomura A, Matsuda T, Suzuki R, Fukuhara A, Osakabe N, Umezaki H, Endo J, Shinagawa K, Sugita Y and Fujiwara H 1982 *Phys. Rev. Lett.* **48** 1443

[3] Altshuler B L, Arovo A G, Spivak B Z, Sharvin D Y and Sharvin Y V 1982 *JETP Lett.* **35** 588

[4] Webb R A, Washburn S, Umbach C P and Laibowitz R B 1985 *Phys. Rev. Lett.* **54** 2696

[5] Tonomura A, Osakabe N, Matsuda T, Kawasaki T, Endo J, Yano S and Yamada H 1986 *Phys. Rev. Lett.* **56** 792

[6] Lee P A and Stone A D 1985 *Phys. Rev. Lett.* **55** 1622

[7] Stone A D 1985 *Phys. Rev. Lett.* **54** 2692

[8] Lee P A, Stone A D and Fukuyama H 1987 *Phys. Rev.* B **35** 1039

[9] Vila L, Giraud R, Thevenard L, Lemaître A, Pierre F, Dufouleur I, Mailly D, Barbara B and Faini G 2007 *Phys. Rev. Lett.* **98** 027204

[10] Umbach C P, Washburn S, Laibowitz R B and Webb R A 1984 *Phys. Rev.* B **30** 4048

[11] Tserkovnyak Y and Halperin B I 2006 *Phys. Rev.* B **74** 245327

[12] Liang W J, Bockrath M, Bozovic D, Hafner J H, Tinkham M and Park H 2001 *Nature* **411** 665

[13] Bachtold A, Strunk C and Nussbaumer T 1999 *Nature* **397** 673

[14] Schöenberger, Bachtold A and Strunk C 1999 *Appl. Phys.* A **69** 283

[15] Fedorov G, Lassagne B, Sagnes M and Raquet B 2005 *Phys. Rev. Lett.* **94** 66801

[16] Langer L, Bayot V and Grivei E 1996 *Phys. Rev. Lett.* **76** 479

[17] Roche S and Saito R 2001 *Phys. Rev. Lett.* **87** 246803

[18] Man H T and Morpurgo A F 2005 *Phys. Rev. Lett.* **95** 026801

[19] White C T and Todorov T N 1998 *Nature* (London) **393** 240

[20] Taylor J, Guo H and Wang J 2001 *Phys. Rev.* B **63** 245407

[21] Xue Y Q, Datta S and Ratner M A 2002 *Chem. Phys.* **281** 151

[22] Zhang J X, Hou S M, Li R and Qian Z K 2005 *Nanotech.* **16** 3057

[23] Hou S M, Li R, Qian Z K and Zhang J X 2005 *J. Phys. Chem.* A **109** 8356

[24] Ning Z Y, Chen J Z, Hou S M, Zhang J X, Liang Z Y, Zhang J and Han R S 2005 *Chin. Phys. Lett.* **22** 1634

[25] Hod O, Rabani E and Bare R 2006 *Acc. Chem. Res.* **39** 109

[26] London 1937 *J. Phys. Radium.* **8** 397

[27] Ditchfield 1974 *Mol. Phys.* **27** 789

[28] Chen J Z, Zhang J and Han R S 2008 *Chin. Phys. Lett.* **25** 1060